Supplementary Figures

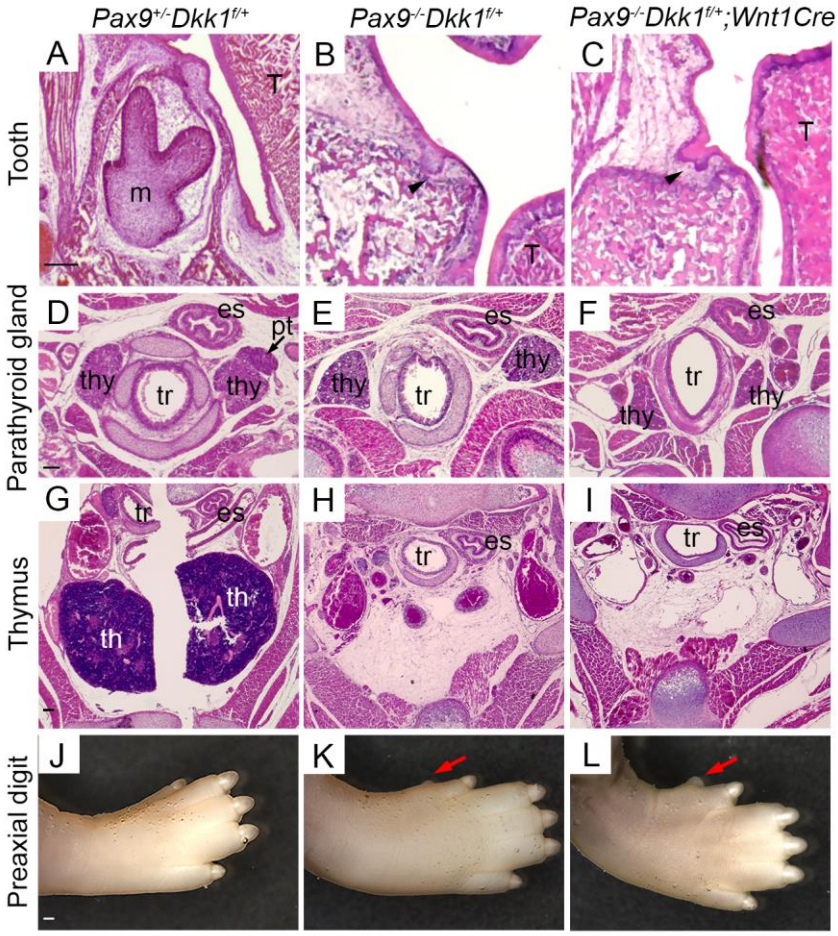

Figure S1. Reducing *Dkk1* in compound mutants of *Pax9*$^{-/-}$*Dkk1*$^{f/+}$*;Wnt1Cre* failed to rescue the defects of tooth organs, parathyroid glands, thymus and hind limb in *Pax9*$^{-/-}$ embryos. (A-C) H&E staining of sections through developing 1st molar in P0 pups. Compared with late bell stage in *Pax9*$^{+/-}$*Dkk1*$^{f/+}$ (A), tooth development arrested at bud stage in *Pax9*$^{-/-}$*Dkk1*$^{f/+}$ (B, black arrowhead) while the 1st molar advanced to early cap stage in *Pax9*$^{-/-}$*Dkk1*$^{f/+}$*;Wnt1Cre* (C, black arrowhead). (D-F) H&E staining of sections through thyroid in P0 embryos. Parathyroid gland is near the dorsolateral border of the thyroid lobe in *Pax9*$^{+/-}$*Dkk1*$^{f/+}$ samples (D, black arrow) but missing in *Pax9*$^{-/-}$*Dkk1*$^{f/+}$ (E) and *Pax9*$^{-/-}$*Dkk1*$^{f/+}$*;Wnt1Cre* embryos (F). (G-I) H&E staining of sections through thymus position in P0 embryos. Compared with the dark-stained thymus in *Pax9*$^{+/-}$*Dkk1*$^{f/+}$ samples (G), *Pax9*$^{-/-}$*Dkk1*$^{f/+}$ (H) and *Pax9*$^{-/-}$*Dkk1*$^{f/+}$*;Wnt1Cre* embryos (I) showed lack of thymus. (J-L) The ventral views of hind limb. In comparison

to the normal digits in *Pax9*$^{+/-}$*Dkk1*$^{f/-}$ samples (J), *Pax9*$^{-/-}$*Dkk1*$^{f/+}$ (K) and *Pax9*$^{-/-}$*Dkk1*$^{f/+}$*;Wnt1Cre* embryos (L) had extra-formed digit (red arrows in K and L). es, esophagus; m, molar; pt, parathyroid gland; T, tongue; th, thymus; thy, thyroid; tr, trachea. Scale bar represents 100µm.

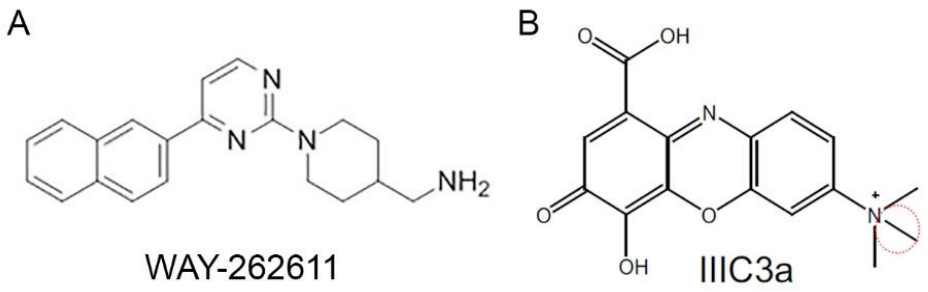

Figure S2. The structure formula of Wnt agonists used for treatments. (A) Dkk1 inhibitor, WAY-262611; (B) Dkk inhibitor II, IIIc3a (Pelletier et al., 2009; Li et al., 2012).

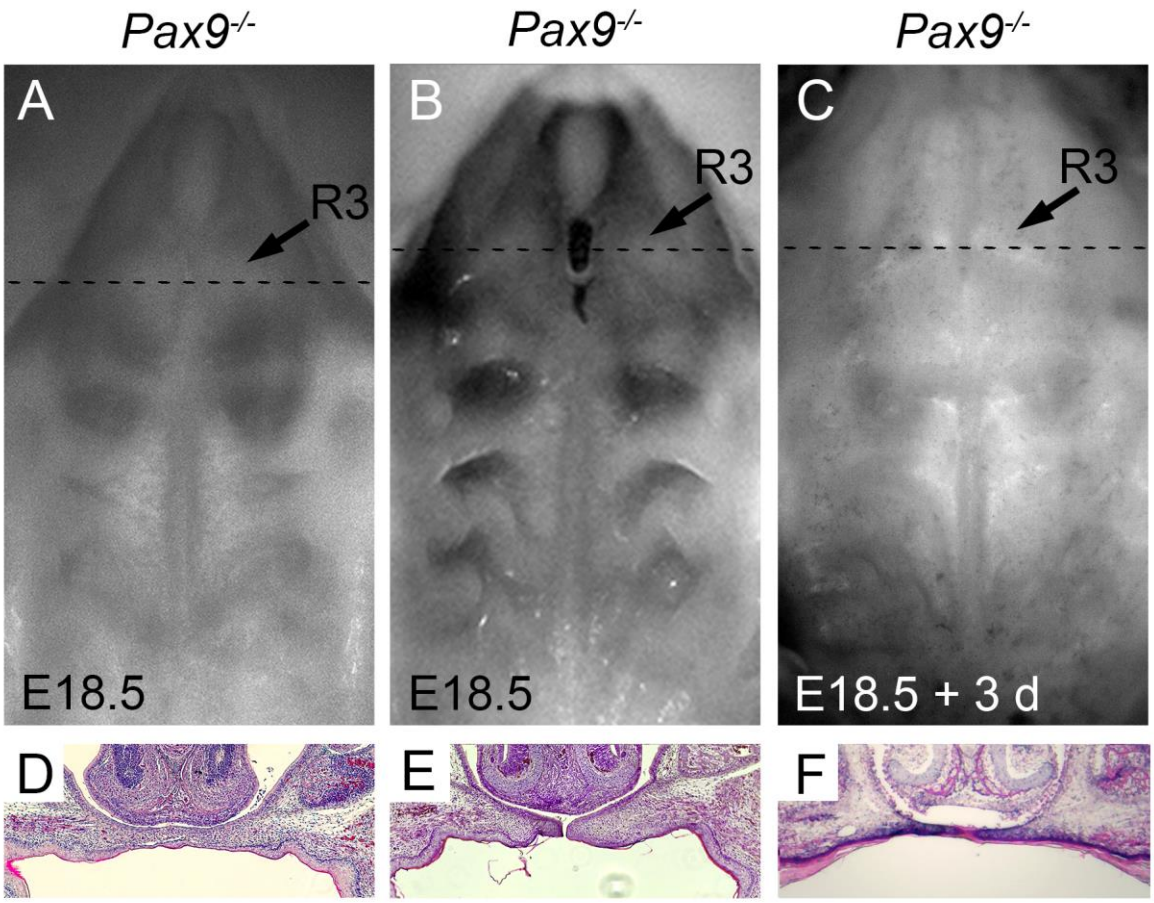

Figure S3. The residual fusion defects in the treated *Pax9*$^{-/-}$ samples were rescued after 3 days of culture. The whole mount view of palates treated with WAY-262611 *in-utero* (A, B) and with additional 3 days of culture after WAY-262611 *in-utero* treatment (C). 60% (11 in 18) *Pax9*$^{-/-}$ embryos showed full closure of palate shelves (A) and 40% (7 in 18) *Pax9*$^{-/-}$ embryos showed residual fusion defects between primary and secondary palate (B). The residual fusion defects were resolved *in-vitro* after culture for 3 days (n=5) (C). Dashed line indicates the position of section in D, E, F, respectively. Black arrows point the position of the 3rd ruga (R3). HE staining of frontal sections through palates showed fully closure (D), small gap at the 3rd ruga (E) and the gap disappeared after 3 days of culture (F).

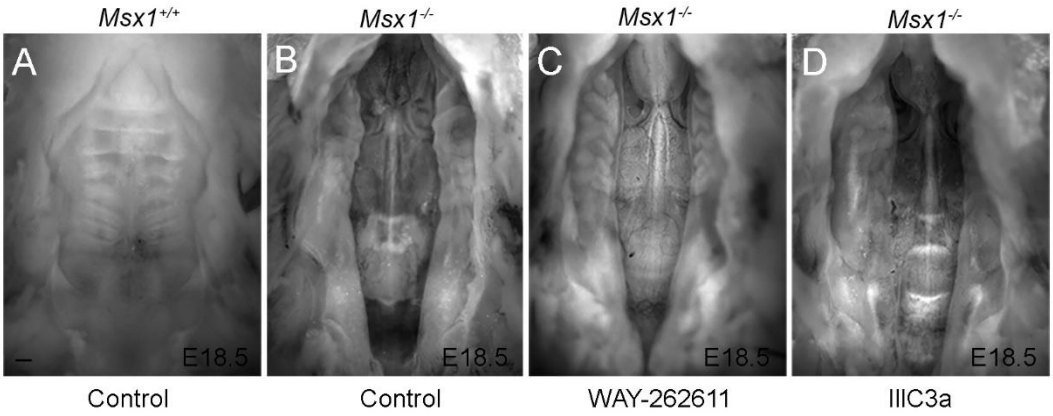

Figure S4. The treatments with Wnt signaling agonists didn't rescue cleft palate in *Msx1*$^{-/-}$ embryos. Compared with intact palate in *Msx1*$^{+/+}$ embryo (A), all the *Msx1*$^{-/-}$ embryo (B), WAY-262611 treated *Msx1*$^{-/-}$ embryos (C, 15 samples) and IIIc3a treated *Msx1*$^{-/-}$ embryos (D, 34 samples) showed 100% penetrance of the complete cleft palate.

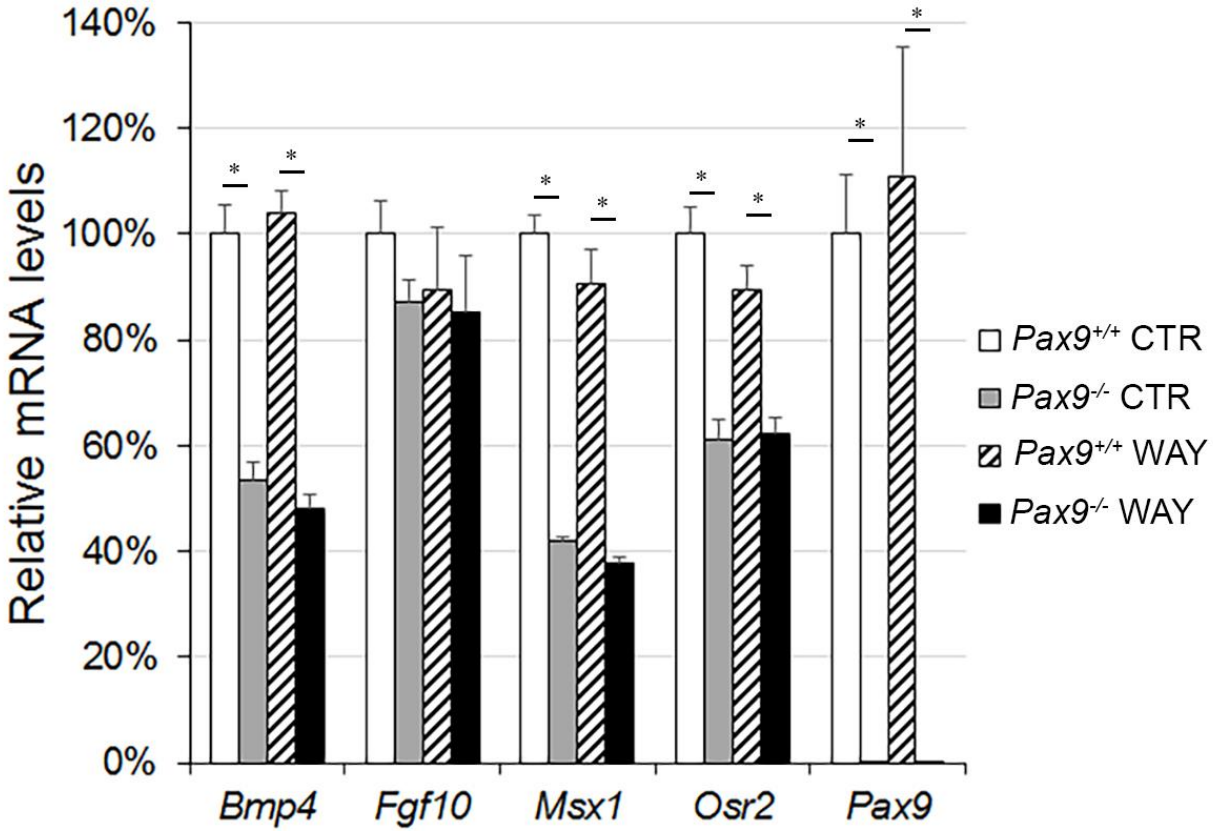

Figure S5. Quantitative RT-PCR analysis of gene expression of known Pax9 targets from control and WAY-262611 treated groups. In *Pax9*$^{-/-}$ samples, the expression levels of endogenous *Osr2, Msx1* and *Bmp4* were significantly reduced while *Fgf10* mRNA was moderately decreased. Treatment with Wnt signaling agonist WAY-262611 did not appear to restore levels of *Bmp4, Msx1, Fgf10* and *Osr2* expression. Error bars indicate s.e.m., * $P < 0.05$. CTR, control treatment; WAY, WAY-262611 treatment.

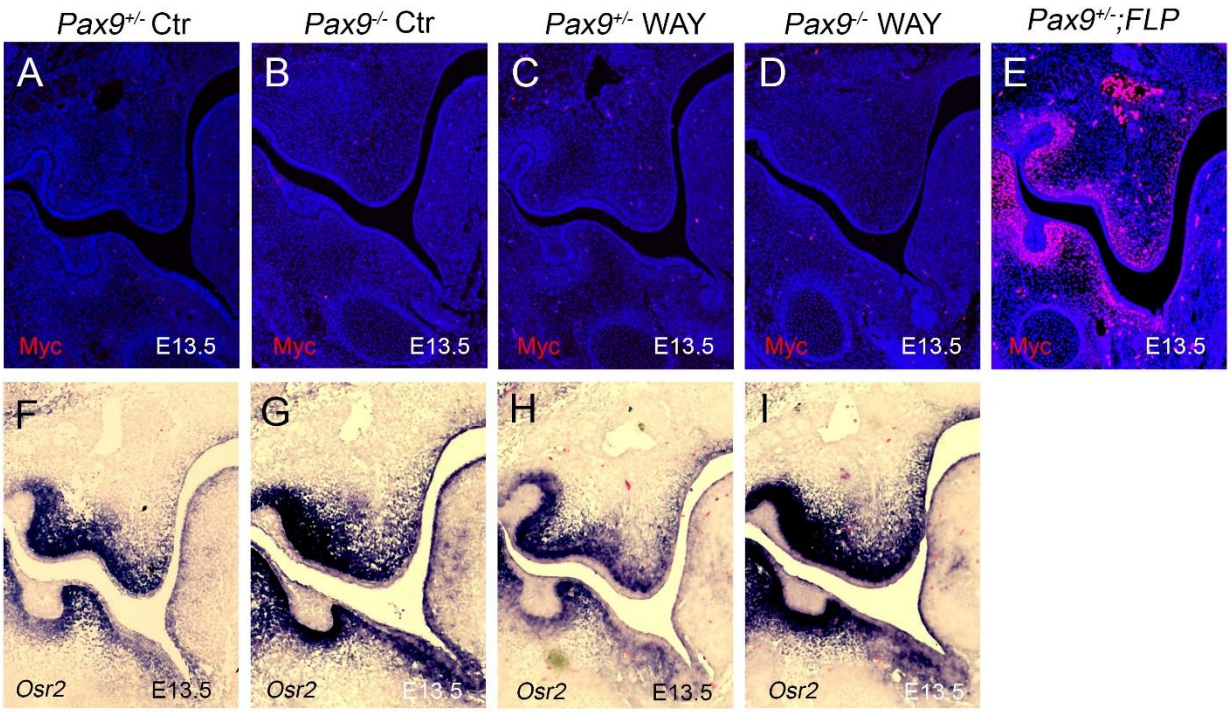

Figure S6. The knock-in *Myc-Osr2* was not translated into protein in the palate after WAY-262611 treatment. (A-E) Lack of detection of Myc-Osr2 protein in E13.5 palate frontal sections in WAY-262611 treated embryos using anti-Myc antibody. No Myc-staining was detected in *Pax9*$^{+/-}$ or *Pax9*$^{-/-}$ samples with control or WAY-262611 treatment (A-D). *Pax9*$^{+/-}$*;FLP* (also named *Pax9*^{Osr2KI} in Zhou et al., 2011) sample was used as the positive control to show the strong and specific Myc-staining, in which samples *Myc-Osr2* was translated into protein (E). (F-I) *In-situ* hybridization in E13.5 palate frontal sections using *Osr2*-specific probe. Though stronger *Osr2* signals were detected in *Pax9*$^{-/-}$ samples (G, I) than *Pax9*$^{+/-}$ samples (F, H), representing the transcription of extra copy of transgenic *Osr2*, there is no significant increase of Osr2 expression after WAY-262611 treatment (comparing H with F, I with G). Anti-Myc antibody staining in red and *in-situ* hybridization signals are shown in blue. Ctr, control treatment; WAY, WAY-262611 treatment.

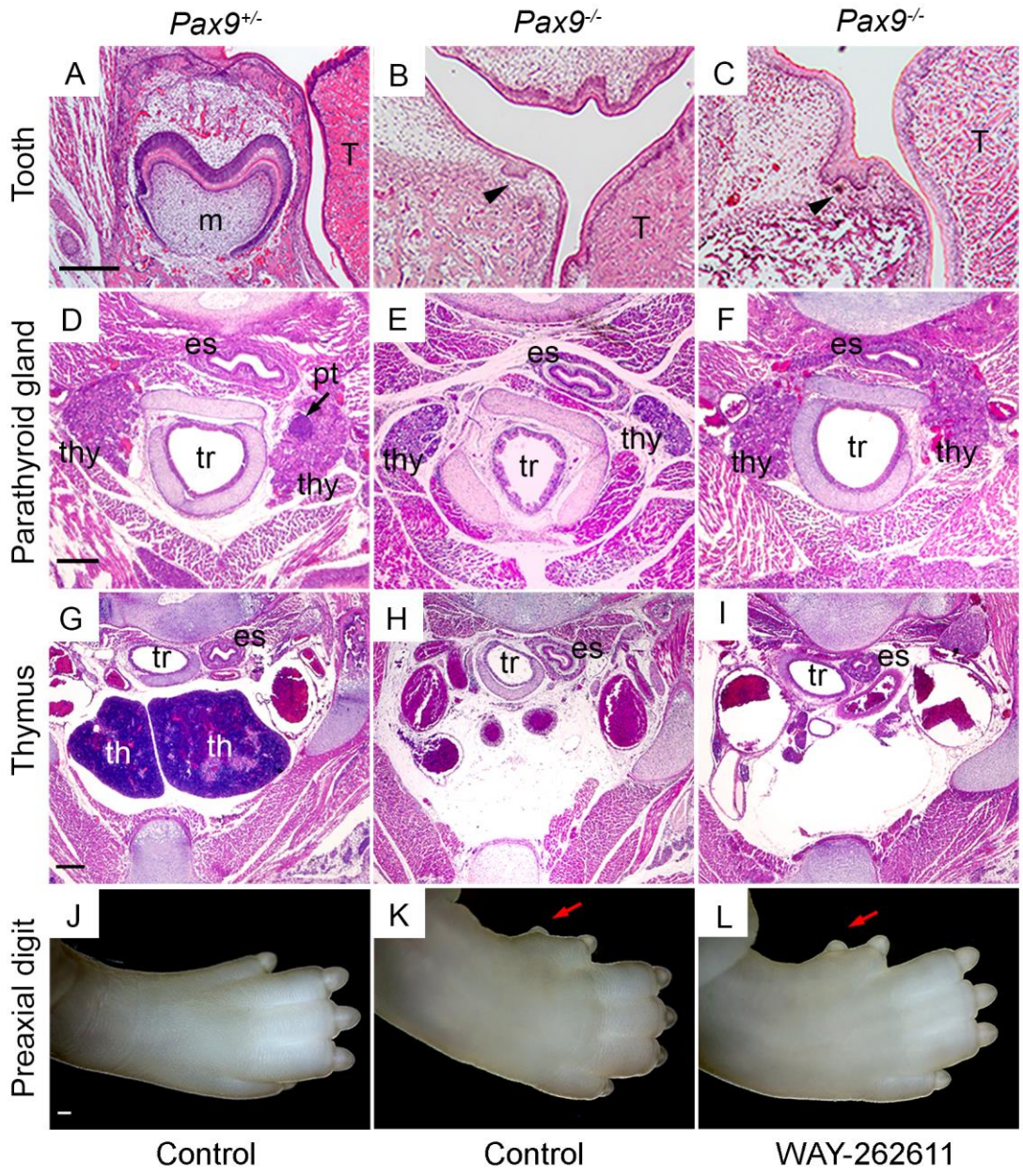

Figure S7. Wnt agonist therapies failed to rescue the defects of tooth organs, parathyroid glands, thymus, and hind limb in *Pax9*$^{-/-}$ embryos. (A-C) H&E staining of sections through developing 1st molar at E18.5. Compared with late bell stage in *Pax9*$^{+/-}$ (A), tooth development arrested at bud stage in *Pax9*$^{-/-}$ (B, black arrowhead) while the 1st molar advanced to early cap stage in WAY-262611 treated *Pax9*$^{-/-}$ (C, black arrowhead). (D-F) H&E staining of sections through thyroid of E18.5 embryos. Parathyroid gland is near the dorsolateral border of the thyroid lobe in *Pax9*$^{+/-}$ samples (D, black arrow) but missing in *Pax9*$^{-/-}$ embryos without (E) or with (F) WAY-262611

treatment. (G-I) H&E staining of sections through thymus position in E18.5 embryos. Compared with the dark-stained thymus in *Pax9*$^{+/-}$ samples (G), *Pax9*$^{-/-}$ embryos without (H) or with (I) WAY-262611 treatment showed lack of thymus. (J-L) The ventral views of hind limb. In comparison to the normal digits in *Pax9*$^{+/-}$ samples (J), *Pax9*$^{-/-}$ embryos without (K) or with (L) WAY-262611 treatment had extra-formed digit (red arrows in K and L). es, esophagus; m, molar; pt, parathyroid gland; T, tongue; th, thymus; thy, thyroid; tr, trachea. Scale bar represents 200μm.

Supplementary Table 1:
Primers for Quantitative RT-PCR

Name	Sequence	Name	Sequence
Bmp4-QF	GAGGGATCTTTACCGGCTCC	*Cited1-QF*	TCGCTTCGTCCGTACCTCAG
Bmp4-QR	GTTGAAGAGGAAACGAAAAGCAG	*Cited1-QR*	CTCCTGGTTGGCATCCTCCTT
Dkk1-QF	AACTACCAGCCCTACCCTTG	*Gbx2-QF*	GCAACTTCGACAAAGCCGAG
Dkk1-QR	TCTGGGATATCCATCCCCCG	*Gbx2-QR*	GACAGCCCCGACGAGC
Dkk2-QF	TACTCTTCCAAAGCCAGACTCCA	*Fgf4-QF*	AAGCTCTTCGGTGTGCCTTT
Dkk2-QR	CCTCATTCTTCCGCATTCCA	*Fgf4-QR*	CGGAGGGTCACAGTCTAGGA
Lef1-QF	GAAATCATCCCAGCCAGCAA	*Phox2b-QF*	GTACGCCGCAGTTCCATACA
Lef1-QR	GGGCATCATTATGTAGCCAGAGTA	*Phox2b-QR*	CTGCTTGCGAAACTTAGCCC
Tfap2b-QF	TACAGACAGCGGAGTCCTGA	*Hand2-QF*	CACCAGCTACATCGCCTACC
Tfap2b-QR	CATCGTGCCGGTCCTCATAG	*Hand2-QR*	TCTCATTCAGCTCTTTCTTCCTCT
Msx1-QF	CGGCCATTTCTCAGTCGG	*Ascl1-QF*	TCTCGTCCTACTCCTCCGAC
Msx1-QR	CTTGCGGTTGGTCTTGTGC	*Ascl1-QR*	ATTTGACGTCGTTGGCGAGA
Msx2-QF	ACACCCTTCACCACATCCCA	*L1cam-QF*	GCTCCTCATCCTGCTCATCC
Msx2-QR	TTCCGCCTCTTGCAGTCTTT	*L1cam-QR*	TCTCCAGGGACCTGTACTCG
Pax9-QF	TATTCTGCGCAACAAGATCG	*Osr2-QF*	TCTTTACACATCCCGCTTCC
Pax9-QR	GGTGGTGTAGGCACCTTAGC	*Osr2-QR*	GGAAAGGTCATGAGGTCCAA
Fgf10-QF	TTTGAGCCATAGAGTTTCCCC	*Gapdh-F*	TGGAGCCAAAAGGGTCA
Fgf10-QR	CGGGACCAAGAATGAAGACTG	*Gapdh-R*	CTTCTGGGTGGCAGTGA